Jurnal Teknologi

Full paper

Load-deformation Behaviour of Eccentrically Loaded SSTT-confined High Strength Concrete Columns

Ma Chau Khun, Abdullah Zawawi Awang*, Wahid Omar

Faculty of Civil Engineering, Universiti Teknologi Malaysia, 81310 UTM Johor Bahru, Johor, Malaysia

*Corresponding author: abdullahzawawi@utm.com.my

Article history

Received: 10 November 2014
Received in revised form:
23 January 2015
Accepted: 12 April 2015

Graphical abstract

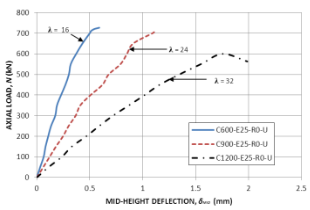

Abstract

The application of steel-straps confinement or better known as steel-strapping tensioning technique (SSTT) has been proven to be effective in increasing the strength and ductility of High-Strength Concrete (HSC) column comparable to Fiber-Reinforced Polymer (FRP). However, most of the research of confined HSC column has mainly concentrated on concentric loading. In actual practical condition, most of the columns are subjected to eccentric loading. The scarcity of the experimental data for eccentric loaded confined HSC column has prevented the potential use of this type of structure element. In this paper, five HSC columns were tested. The specimens were SSTT-confined and tested with 25mm and 50 mm eccentric loading. The results show that SSTT confinement can increase the strength and deformability of high-strength concrete column, although the strain gradient reduces the confining efficiency. Therefore, smaller capacity enhancement factor should be used in eccentrically loaded SSTT-confined HSC columns compared to concentrically loaded columns. Furthermore, the non-linear theoretical model established in this study can be used for templates for future work on SSTT-confined HSC columns.

Keywords: Steel-straps confinement; high-strength concrete; SSTT; load-deformation behaviour

© 2015 Penerbit UTM Press. All rights reserved.

1.0 INTRODUCTION

HSC has gained its popularity due to its greater compressive strength compared to Normal-Strength concrete (NSC). With the development of technology, the use of HSC concrete members has been proven to be popular in terms of economy; higher strength, better stiffness and more durable[1,2,3,4,5,6]. However, it is generally known that, with the increase of concrete strength, a relatively more brittle failure occurs. The lack of ductility in HSC members results in sudden failure without warning, which hindered the full potential use of it in confidence[7].

External confinement has been focused as one of the confinement method which was proven to be effective in enhancing the structural properties of HSC[8]. These higher strengths are achieved as the result of the lateral pressures, applied by the external confinement and limiting the lateral expansion of the concrete column. The confinement effect initiated by the lateral expansion of the column under loading, improved the stiffness of column. As a result, the confined HSC column can sustain larger axial loads as compared to its unconfined counterparts.

In practice, column loaded by pure axial load is rarely occurred. The bending effect always exist even the column was designed only to carry axial load. This is likely due to the unintentional load eccentricities or error in construction. The strain gradient caused by the eccentric loading further reduced the confinement effects[9]. Therefore, the studies of confined HSC column subjected to eccentric load are essential for practical application.

2.0 LITERATURE REVIEW

The confinement increases ductility and compressive strength of concrete under compression by resisting the lateral dilation due to the Poisson's effect upon loading. The confining effect is deemed to be insignificant or negligible until a particular stress due to the Poisson's effect is reached and initiated the confinement. It was reported that the confinement does not take effect initially, but when the stress is about 60% of the corresponding maximum concrete strength, it was perfectly confined[6]. At this load stage, internal stress distribution of the concrete under compression has been completed and the energy stored within the confined concrete is adequate to cause the formation of the micro-cracking (lateral dilation of concrete was caused by the formation of micro-cracking) and thus initiating the confining effects.

In the confinement of HSC plain columns, confinement enhances the ductility of the members by restoring the energy within the confined core concrete under compression, and thus further extending the post-elastic strain of the concrete.

Several researches have been carried out to investigate the behavior of column subjected to eccentric load to simulate real construction situation. Hadi (2005) tested HSC column of 50 mm eccentric load[10]. The eccentricities were achieved by offsetting 50 mm from the neutral axis by employing eccentric load plate and adaptive plate. It was found that, the eccentricities affect the deformability and load carrying capacity of HSC column. Hadi and Li (2004) externally confined the HSC column with FRP and tested under eccentric load[11]. The column was made with haunches at both ends in order to facilitate the application of eccentric load. It was observed that, the load carrying capacity was significantly reduced as the eccentricity increased. Hamdy and Radhouane (2009) tested numbers of concrete filled FRP tube (CFFT) columns under eccentric load[12]. The results, again, give the same conclusion as the increased in eccentricities decreased the ultimate load capacity and increased the horizontal and axial deformation of the CFFT columns. Other tests carried out by Parvin & Wang (2001) proved that, the level of confinement, provided by different layers of FRP jacket, also influenced the performance of HSC columns[9]. For eccentric loaded HSC column, with certain level of confinement, the load carrying capacity of column significantly improved.

3.0 EXPERIMENTAL PROGRAMME

The main objective of the experimental program is to investigate the behavior of externally confined HSC column subjected to eccentric loading and to evaluate the effectiveness of steel-straps as confining material. In this study, the testing variables selected are: (1) confinement ratio: spacing of steel-straps and number of confinement layers, (2) eccentricities of loading.

Five HSC columns were tested under eccentric loading. Each column was designed to have a diameter of 150 mm and overall length of 600 mm. The dimensions of the specimen were selected to be compatible with the capacity of the testing machine. Four longitudinal bars (10 mm ribbed bar, 460 MPa) were equally distributed around the circumference of each column. The longitudinal bars were tied with equally-spaced stirrups (R6-300 mm c/c, 250 MPa). The testing matrix is shown in Table 1.

Table 1 Testing matrix on column specimens

Column	Diameter (mm)	Length (mm)	Eccentricities (mm)	Configurations
C600-E25-R0.5-C	150	600	25	Plain column
C600-E25-R0.5-1L(20)	150	600	25	One-layered, 20 mm spacing
C600-E25-R0.5-1L(40)	150	600	25	One-layered, 40 mm spacing
C600-E25-R0.5-2L	150	600	25	Two-layered, 40 mm spacing
C600-E50-R0.5-1L(20)	150	600	50	One-layered, 20 mm spacing

Figure 1 shows the test set-up. Eccentric load was subjected to the column by eccentric load plate and knife edge. The test stopped once the load plate contact with the adaptive plate. Dartec 2000 kN compression machine was used in this experiment. Three LVDTs were used to measure the lateral deflection of the columns. One LVDT was placed laterally at the mid-height of the column. Another two LVDTs were placed approximately 150 mm from the LVDT of mid-height. All specimens were tested under compressive load using a displacement control testing machine with the capacity of 2000 kN with constant rate of 0.4 mm/min.

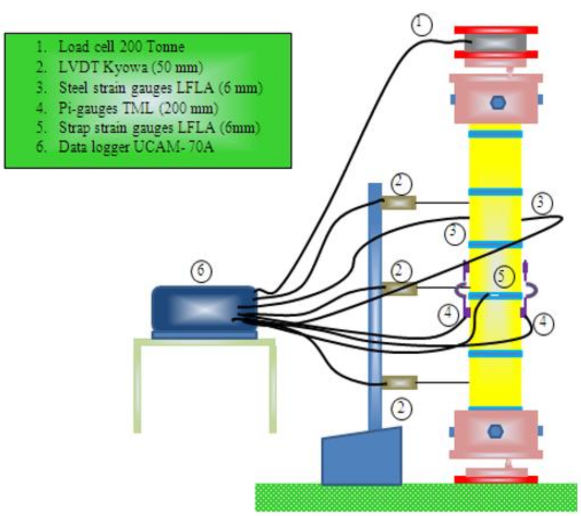

Figure 1 Schematic of Test Set up and Instrumentation for Eccentric Test

4.0 NUMERICAL MODELLING

A theoretical model is developed to analysis slender SSTT-confined HSC columns subjected to eccentric loads. The model simulates the second-order moment distribution experienced by slender SSTT-confined HSC column by generating axial load-moment curvature path. The calculation of load-deflection curve at each discrete point of column is obtained by numerical integration method which was originally proposed by Newmark (1943)[13]. The analysis is conducted with the aid of MATLAB 7.6.

Material Properties

For SSTT-confined HSC, the confinement model proposed by Mander *et al.* (1988)[14] is adopted with slight modification. Their model utilized the equations originally developed by Popovics (1973)[12] for stress-strain response of unconfined concrete. The concrete stress, f_{ci} at a given strain, ε_{ci} is as below:

$$f_{ci} = \frac{f'_{cc} x . r}{r - 1 + x^r} \tag{1}$$

where, $x = \varepsilon_{cc} / \varepsilon'_{cc}$, $r = E_c / (E_c - E'_{sec})$, ε_{cc} is the axial compressive strain of concrete given by $\varepsilon_{cc} = [1 + 5\left(\frac{f'_{cc}}{f}\right) - 1]$, ε'_{cc} is the strain corresponding to f'_{cc}, E_c is the tangent modulus of elasticity of concrete, estimated to be 22700 $\sqrt{f'_{cc}/19.6}$ (MPa) in this model, E'_{sec} is the secant modulus of confined concrete at peak stress, given by $E'_{sec} = f'_{cc} / \varepsilon'_{cc}$ (MPa) and f_{co} is the concrete compressive strength. The confined concrete strength, f'_{cc} is determined based on the empirical equation proposed by Abdullah (2013)[7]:

$$f'_{cc} = f_{co} \times 2.62\left(\rho_s \frac{f_y}{f}\right) \tag{2}$$

where ρ_s is the volumetric ratio, given by V_s/V_c, f_y and V_s are the yield strength and volume of steel straps, respectively. Meanwhile V_c is the volume of confined concrete. The peak strain ε'_{cc} is calculated based on empirical equation also from Abdullah (2013)[7]:

$$\varepsilon'_{cc} = \varepsilon_{co} \times 11.60\left(\rho_s \frac{f_y}{f}\right) \quad (3)$$

where ε_{co} is the ultimate strain of HSC. In Abdullah's empirical stress-strain model (Abdullah, 2013)[7], this value is estimated to be 0.004.

$$f_y = E_s.\varepsilon_s\,;\; 0 < \varepsilon_s < \varepsilon_y \quad (4a)$$

$$f_y = f_y\,;\;\; \varepsilon_s \geq \varepsilon_y \quad (4a)$$

where E_s is the elastic modulus of steel estimated to be 200 GPa in this paper. ε_s is the strain of steel and ε_y is the yield strain of steel estimated to be 0.0023.

Numerical Integration of Column Deflection

Once the moment-curvature relationships of the section are obtained, the lateral deflection of the column can be calculated using numerical integration. In prior research, this analysis method has been used in the analysis of RC columns[16,17], steel column[18], composite column[19,20]and FRP-confined RC column[21]. The curvature, $ø$ is assumed to be second order derivative of the lateral deflection, δ of the column. The relationship between the curvature, ø and the lateral deflection, δ can be expressed by using central difference equation as shown below:

$$\delta_{m+1} - 2\delta_m + \delta_{m-1} = -ø_m \times dl^2 \quad (5)$$

where δ_m and $ø_m$ are the lateral displacement and curvature at m-th grid point respectively. m is the index of grid point given by m = 1, 2, 3, …. 31. Meanwhile, dl is the value of column's total length divided by m.

In generating the load-deflection curve, the axial load, N_{step} is increased incrementally and the corresponding deflection at each discrete point along the column length, L is calculated. At a given axial load, N_{step}, axial load- moment- curvature relationship is first developed. The first-order moment can be calculated as:

$$M_{f,step} = N_{step} \times e_m \quad (6)$$

where $M_{f,\mathrm{step}}$ and e_m are the first-order moment and the eccentricity at the m-th point respectively. The second-order moment, $M_{s,\,step}$ can be expressed as:

$$M_{s,step} = N_{step} \times \delta_m \quad (7)$$

Hence, the total moment can be calculated by summarizing $M_{f,step}$ and $M_{s,step}$, given by:

$$M_{step} = M_{f,step} + M_{s,step} = N_{step} \times (e_m + \delta_m) \quad (8)$$

To start the calculation process, value of δ_2 has to be assumed. In this paper, the value for δ_2 is first suggested to be zero for trial purpose. The value for $ø_2$ can then be retrieved from the axial load-moment-curvature relationship prescribed in the previous section once the moment, $M_{2,step}$ is obtained. It should be noted that the value for M_2 can be calculated based on equation 8 with assumed value of δ_2 equal to zero. Once the $ø_2$ and M_2 are known, the value for next discrete point, δ_3 can then be calculated. With the repetition of the above procedure from one discrete point to another, the lateral deflection of the column can be calculated. However, the lateral deflection only considered as valid if it satisfied the condition below:

$$\delta_{(m+1)} = 0 \quad (9)$$

It should be noted that the values for both column ends, δ_1 and $\delta_{(m+1)}$ must be equal to zero. This is due to the assumption that both end of the loaded column must not been deflected. In this paper, the first trial value $\delta_2 = 0$ has resulted in negative value for $\delta_{(m+1)}$. The value of δ_2 is adjusted to a larger value to satisfied condition 9. In present analysis, the solution for the lateral deflection at a given load is stopped when the calculated δ_{31} has an absolute value less than 0.0001 mm. Detail procedure and verification of the numerical analysis can be found in Ma *et al*. (2014)[22].

5.0 RESULT AND DISCUSSIONS

Similar behaviour was found for all the confined columns under eccentric loading. Sounds of snapping of the steel-straps were heard near the ultimate load. It should be noted that no post-peak behaviour was observed for all tested column. The failure of the columns was generally marked by crushing of the concrete in the compression area. There was no indication of reinforcement buckling until the concrete is completed crushed. Increases in the lateral deflection for confined columns were observed resulted in the concrete failing in compression and rupturing of the steel straps. The signs of distress of steel-straps confinement were the heard sounds and large lateral deflections of columns. The typical failure modes of unconfined and confined HSC columns were shown in Figure 2. The results from the experiment are shown in Table 2.

Table 2 Results of tested specimens

Column	Ultimate load (kN)	Ultimate mid-height deflection (mm)
C600-E25-R0.5-C	726.9	0.59
C600-E25-R0.5-1L(20)	605.4	0.43
C600-E25-R0.5-1L(40)	860	0.80
C600-E25-R0.5-2L	1020.5	0.90
C600-E50-R0.5-1L(20)	565	0.57

(a) Unconfined (b) Confined

Figure 2 Typical failure modes for eccentrically loaded columns

Load-deformation Behaviour

The tested load-deformation diagrams are shown in Figure 3. In Figure 3, the experimental results were compared with numerical analysis results. It can be seen that as the load increases, larger deflection was observed for column confined with higher confinement ratio. It should be noticed that the columns with higher confinement ratio achieved bigger lateral deflection. This is mainly due to the confinement increases the compressive strain of the column. This results in higher curvature and consequently increases in lateral deflection. As can be seen in Figure 3(c), the lateral deflection achieved by the confined column is about 35.6% higher than the unconfined counterpart. As for confined column with low confinement ratio, similar load-deflection curves were observed for both confined and unconfined column as can be seen in Figure 3(a). This is mainly due to this configuration yield no significant effects in increasing the concrete strain or curvature. It is worth noting that for eccentrically loaded HSC columns, certain confinement limit should be imposed to ensure the effectiveness of the confinement used. However, some discrepancies were found between the numerical and experimental results as can be witnessed in Figure 3(b) and 3(e). One possible reason is that the eccentricity has certain effect on determining the ultimate axial strain of the confined concrete, which is not considered in this model. However, in general it was found that the proposed model is sufficiently accurate in predicting the load-deformation behaviour of the confined columns.

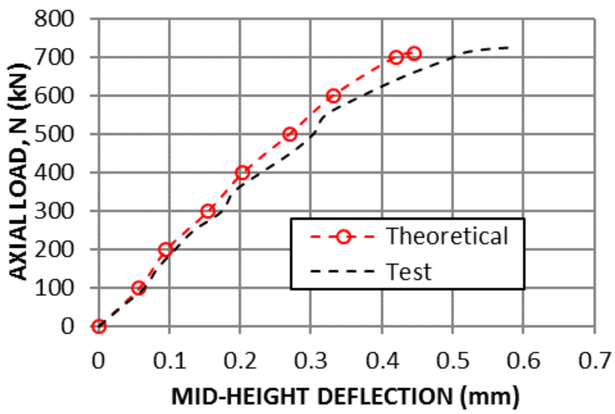

(a) C600-E25-R0.5-C

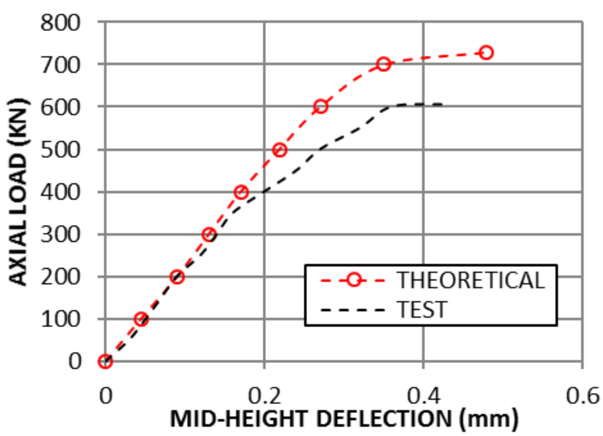

(b) C600-E25-R0.5-1L(20)

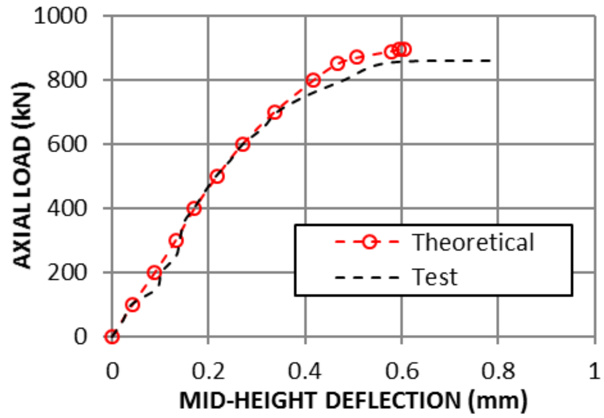

(c) C600-E25-R0.5-1L(40)

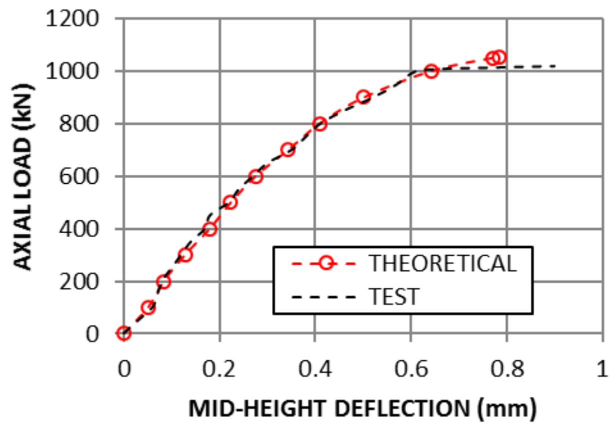

(d) C600-E25-R0.5-2L

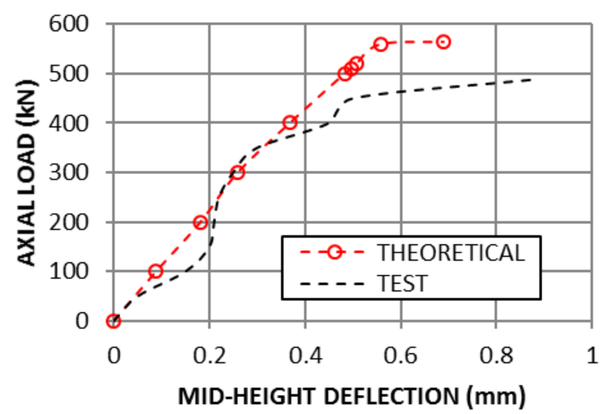

(e) C600-E50-R0.5-1L(20)

Figure 3 Comparison of load-deflection diagrams of experimental and numerical analysis results

■6.0 CONCLUSIONS

Steel-straps confinement is effective in increasing the ultimate load of eccentrically loaded column. The ultimate load is increased with the increased of the confinement ratio. Higher confinement ratio can be obtained by either narrowing the space of steel straps or increasing the number of layers. The confinement significantly improved the deformability of HSC columns compared to unconfined counterpart. For higher confinement ratio, the confined column presented approximately 35.6% higher deflection compared to unconfined column. Certain limit on the confinement ratio should be imposed when utilizing steel-straps confinement. No significant effects can be made beyond this limit. The theoretical model is compared against the experimental results, which correlated well with numerical analysis results. The assumptions of the pinned-fixed conditions and effective column length of in the experimental test seem to be reasonable.

Notation

The following symbols are used in this paper:

A_{si} = corresponding cross-sectional area of longitudinal steel bar
A_{conc} = total cross-sectional area of column
A_{st} = total cross-sectional area of longitudinal bars
D = diameter of column section
dl = thickness of each layer of discretized column section
dL = length of column segmented unit
d_{si} = location of longitudinal tensile bar from the extreme concrete fiber
e = load eccentricities
e_m = load eccentricities at a given column grid-point
e_i = column end eccentricities which always has absolute positive value
e_s = column end eccentricities which can be either positive or negative value
E_c = tangent modulus of elasticity of concrete
E'_{sec}= secant modulus of confined concrete at peak stress
E_s = steel elastic modulus
$\boldsymbol{\varepsilon}_{co}$ = Ultimate strain of HSC
$\boldsymbol{\varepsilon}'_{cc}$ = confined concrete's peak strain
$\boldsymbol{\varepsilon}_s$ = strain of steel
$\boldsymbol{\varepsilon}_y$ = yield strain of steel
$\boldsymbol{\varepsilon}_{ci}$ = concrete strain
$\boldsymbol{\varepsilon}_{cc}$ = axial compressive strain of concrete
f_{ci} = concrete stress at a given strain
f_{co} = concrete compressive strength
f_y = yield strength of steel
L = length of column
M_{step} = bending moment at successively incremental loading steps
$M_{f,\ step}$ = first-order moment at a given load step
$M_{s,\ step}$ = second-order moment at a given load step
N_{step} = axial load at successively incremental loading steps
N_{ult} = ultimate load capacity of column under concentric load
$N_{u,\ test}$ = ultimate load from experimental test
$N_{u,\ theo}$ = ultimate load from theoretical analysis
R = radius of column section
s = clear spacing of steel straps
t_s = thickness of steel straps
V_s = volume of SSTT-confinement
V_c = volume of concrete
x = ratio of axial compressive strain to concrete peak strain
xN = neutral axis
y_i = width of *i-th* layer
ρ_s = confinement volumetric ratio
ρ = internal reinforcement ratio
δ_m = lateral deflection at a given column grid-point
δ = lateral deflection
ø = curvature
$\boldsymbol{\sigma}_{si}$ = stress of longitudinal bar at *i-th* layer

Acknowledgement

This research study is sponsored by Ministry of Higher Education of Malaysia through the MyPhd scholarship.

References

[1] Rashid, M. A., Mansur, M. A., and Paramasivam, P. 2002. Correlations Between Mechanical Properties of High Strength Concrete. *Journal of Materials in Civil Engineering*. 14(3): 230–238.
[2] Carrasquillo, P. M., and Carrasquillo, R. L. 1988. Evaluation of the Use of Current Concrete Practice in the Production of High-strength Concrete. *ACI Material Journal*. 85(1): 49–54.
[3] Naik, T. R., Singh, S., and Ramme, B. 1998. Mechanical Properties and Durability of Concrete Made with Blended Fly As. *ACI Material Journal*. 97(2): 136–147.
[4] Ismail, M. A., Budiea, A. M. A., Hussin, M. W., and Muthusamy, K. B. 2010. Effect of POFA Fineness on Durability of High Strength Concrete. *The Indian Concrete Journal*. 84(11): 21–28.
[5] Abdul Rahman, A. S., Ismail, M. A., and Hussain, M. S. 2011. Corrosion Inhibitors for Steel Reinforcement in Concrete. *A Review. Scientific Research and Essays*. 6(20): 4152–4162.
[6] Ismail, M. A., Hamzah, E., Goh, C. G., Abd Rahman, I. 2010. Corrosion Performance of Dual-phase Steel Embedded in Concrete. *Arabian Journal for Science and Engineering*. 35(2A): 81–90.
[7] Abdullah, A. Z. 2013. Stress-strain Behavior of High-strength Concrete With Lateral Pre-tensioning Confinement. Ph.D Dissertation, Universiti Teknologi Malaysia, Malaysia.
[8] Hadi, M. N. S. 2011. External reinforcement of concrete columns. 11th Underground Coal Operators' Conference, University of Wollongong & the Australasian Institute of Mining and Metallurgy. 121–128.
[9] Parvin, A., and Wang, W. 2001. Behavior of FRP Jacketed Concrete Columns Under Eccentric Loading. *Journal of Composites for Construction*. 5(4): 146–152.
[10] Hadi, M. N. S. 2005. Using Fibers to Enhance the Properties of Concrete Column. *Construction and Building Material*. 21: 118–125.
[11] Hadi, M. N. S., J. Li. 2004. External Reinforcement of High Strength Concrete Columns. *Construction and Building Material*. 64: 279–287.
[12] Hamdy, M., and Radhouane, M. 2009. Behavior of FRP Tubes-encased Concrete Columns Under Concentric and Eccentric Loads. *American Composites Manufacturers Association, Composites & Polycon 2009*.
[13] Newmark, N. M. 1943. Numerical Procedure for Computing Deflections, Moments, and Buckling Loads. *ASCE Transactions*. 108: 1161–1234.
[14] Mander, J. B., Priestley, M. J. N., and Park, R. 1988. Theoretical Stress-strain Model for Confined Concrete. *Journal of Structural Engineering*. 114(8): 1805–1826.
[15] Popovics, S. 1973. A Numerical Approach to the Complete Stress-Strain Curves for Concrete. *Cement and Concrete Research*. 3(5): 583–599.
[16] Pfrang, E. O. and Siess, C. P. 1961. Analytical Study of the Behavior of Long Restrained Reinforced Concrete Columns Subjected to Eccentric Loads. Structural Research Series No.214. University of Illinois, Urbana, Illinois.
[17] Cranston, W. B. 1972. Analysis and Design of Reinforced Concrete Columns. Research Report 20, Cement and Concrete Association, UK.
[18] Shen, Z. Y. and Lu, L. W. 1983. Analysis of Initially Crooked, End Restrained Steel Columns. *Journal of Constructional Steel Research*. 3(1): 10–18.
[19] Choo, C. C., Harik, I. E. and Gesund, H. 2006. Strength of Rectangular Concrete Columns Reinforced with Fiber-reinforced Polymer Bars. *ACI Structural Journal*. 103(3): 452–459.
[20] Tikka, T. M. and Mirza, S. A. 2006. Nonlinear Equation for Flexural Stiffness of Slender Composite Columns in Major Axis Bending. *Journal of Structural Engineering, ASCE*. 132(3): 387–399.

[21] Jiang, T. and Teng, J. G. 2012. Behavior and Design of Slender FRP-Confined Circular RC Columns. *Journal of Composites for Construction*. 16(6): 650–661.

[22] Ma, C.K, Abdullah, A.Z, Wahid Omar. 2014. New theoretical model for SSTT-confined HSC Columns. *Magazine of Concrete Research*. 66(2): 1–11.